Int. J. Heat Mass Transfer. Vol. 10, pp. 1179–1194. Pergamon Press Ltd. 1967. Printed in Great Britain

FORCED CONVECTIVE HEAT TRANSFER IN A STRAIGHT PIPE ROTATING AROUND A PARALLEL AXIS

(1ST REPORT, LAMINAR REGION)

YASUO MORI and WATARU NAKAYAMA

Department of Mechanical Engineering, Tokyo Institute of Technology, Meguro-ku, Tokyo

(*Received* 8 *March* 1967)

Abstract—A forced convective heat transfer in a straight pipe rotating around a parallel axis with a large angular velocity has been studied by assuming an effective secondary flow due to buoyancy. Heat-transfer problems studied in this paper are commonly found when cooling electric generators or other rotating machines. Flow and temperature fields are analyzed by dividing them into a flow core region and a thin boundary layer along the wall. The analysis of a fully developed laminar flow under a constant wall temperature gradient condition consists of two parts in this report. The first part is common in various problems with secondary flows and the second part includes points for the present problem. The result shows that both the ratio of resistance coefficients and that of Nusselt numbers to the values for the Poiseuille flow are proportional to $(Ra_r \cdot Re)^{\frac{1}{4}}$. ($Ra_r$, Rayleigh number in the centrifugal field; Re, Reynolds number). The correction coefficients due to the Coriolis effect are also given.

NOMENCLATURE

A, w_1 at the pipe axis;
A', g_1 at the pipe axis;
a, radius of the pipe;
b, $\equiv 1 - (1/\delta_m)\int_0^\delta h\,d\xi$;
C, $\equiv -(\partial P/\partial z)$;
c_p, specific heat of fluid at constant pressure;
D, dimensionless velocity of secondary flow in the core region;
G, $\equiv T_w - T$;
Gr, Grashof number in centrifugal field $\equiv (aH)\omega^2\beta\tau a^4/\nu^2$;
g, $\equiv G/\tau a$;
g_m, $\equiv (T_w - T_m)/\tau a$;
h, polynomial of ξ/δ giving g in the boundary layer;
J, $\equiv 2a^2\omega/\nu$;
k, heat conductivity of fluid;
Nu, Nusselt number $\equiv 2aQ_{wm}/k(T_w - T_m)$;
Nu_0, Nusselt number for symmetrical distributions $= 48/11$;
P, $\equiv (a^2/\nu^2)(p/\rho)$;
Pr, Prandtl number;
p, pressure;
Q_r, Q_ψ, heat flux in the fluid;
Q_w, heat flux at the wall;
q_η, $\equiv Q_r/k\tau$;
q_ψ, $\equiv Q_\psi/k\tau$;
q_w, $\equiv Q_w/k\tau$;
Ra_r, Rayleigh number in centrifugal field $= Gr\,Pr$;
Re, Reynolds number $\equiv 2aW_m/\nu$;
r, radial coordinate in a cross section;
T, temperature;
T_m, mixed mean temperature;
T_w, wall temperature;
U, radial component of velocity, $u \equiv Ua/\nu$;
V, circumferential component of velocity, $v \equiv Va/\nu$;
W, axial component of velocity, $w \equiv Wa/\nu$;

W_m, mean velocity, $w_m \equiv W_m a/\nu$;
Z, axial coordinate, $z \equiv Z/a$.

Greek symbols

β, coefficient of volumetric expansion;
Δ, deviation angle $\equiv \psi - \psi'$;
δ, dimensionless boundary-layer thickness;
δ_T, dimensionless thermal boundary-layer thickness;
ζ, $\equiv \delta_T/\delta$;
H, dimensionless radius of rotation of the pipe axis;
η, $\equiv r/a$;
λ, resistance coefficient $\equiv (-\partial p/\partial Z)2a/\frac{1}{2}\rho W_m^2$;
λ_0, resistance coefficient for Poiseuille distribution $= 64/Re$;
μ, viscosity;
ν, $\equiv \mu/\rho$;
ξ, $\equiv 1 - \eta$;
ρ, density;
τ, temperature gradient along the pipe axis (constant);
$\tau_{z\eta}, \tau_{z\psi}$, dimensionless shearing stress in the axial direction;
ψ, angular coordinate in a cross section whose original line ($\psi = 0$) agrees with the direction of secondary flow in the core region;
ψ', angular coordinate in a cross section whose original line ($\psi' = 0$) passes through the center of a cross section and the axis of rotation;
ω, angular velocity of the pipe.

Suffixes

0, value at the pipe wall (except for λ_0, Nu_0);
1, value in the core region;
m, mean value taken around the periphery ($\psi = -\pi \sim \pi$) (except for g_m, T_m, W_m);
δ, value at $\xi = \delta$;
δ_T, value at $\xi = \delta_T$.

INTRODUCTION

THE COOLING of parts of rapidly rotating machines becomes more and more important, with the increase in working temperature of heat engines or various machines and in the capacity of electric generators or motors. Coolants flowing through the passage inside a rotating body are subjected to a centrifugal field. The body force in a centrifugal field caused by a high speed revolution gives stronger effects on flow resistance and on heat-transfer rate than in a natural gravitational field. The problem discussed in the present paper is a convective heat transfer to a laminar flow with a strong secondary flow caused by the body force in a straight pipe rotating about a parallel axis. This problem, for example, is important for cooling the conductors of armatures with increased capacity and size.

In a rotating pipe, a secondary flow is present due to the body force. Morris [1] analyzes flow and temperature fields by a perturbation method, assuming that a secondary flow is very weak, and the applicable range of its results is narrow. However, for practical uses, it is necessary to know flow resistance and heat-transfer rate under the strong effect of the secondary flow, because in rotating machines centrifugal fields are strong enough to generate an intense secondary flow. Analyses on this case have not been done so far.

A secondary flow increases the flow resistance and also the heat-transfer coefficient. In the present case, the secondary flow is caused by body forces perpendicular to the direction of the main flow. The secondary flow in a curved pipe results from centrifugal force [2–7]. In a heated straight pipe placed horizontally, the secondary flow occurs due to buoyancy force in a gravitational field, when the temperature difference between wall and fluid is finite [8–10]. When the secondary flow caused by various kinds of body force gets strong enough in a pipe flow, in laminar region velocity profiles become quite different from that of the Poiseuille flow, and the velocity and temperature distribu-

tions have a steep gradient in the layer close to the pipe wall and a gentle gradient in the central core part [6]. These characteristic distributions due to a secondary flow show that the effect of the secondary flow is predominant in almost the whole region of the cross section, and the influences of viscosity and heat conduction are mainly restricted in a thin layer adjacent to the pipe wall. For a theoretical study of the cases with the strong secondary flow, the flow and temperature fields may be divided into the boundary-layer region near the pipe wall where the boundary-layer approximation is available, and the flow core region occupying almost the whole part of the cross section [6–10].

The present paper gives an analysis of a heat transfer to a fully developed laminar flow under the condition of constant wall temperature gradient, following the way of analysis developed and reported in the author's papers [6, 7] about heat transfer in curved pipes. Fluids discussed here have Prandtl numbers of about unity or more. A change in fluid density is taken into account only in terms concerning the body force, and changes in physical properties with temperature are neglected. In the first half of this paper, the part of analysis common to problems with secondary flows is discussed. Specific points in the present problem to calculate flow resistances and Nusselt numbers are discussed in the latter part of the paper.

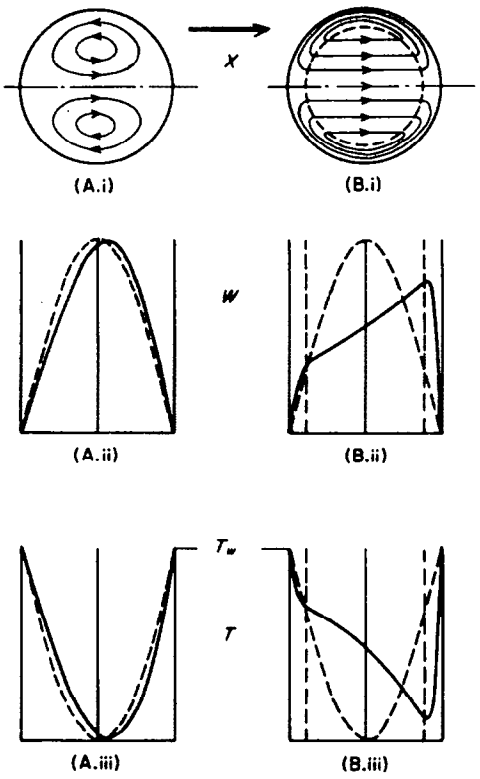

FIG. 1. Flow and temperature fields under the effect of secondary flow.

1. ANALYSIS BY THE BOUNDARY-LAYER APPROXIMATION

1.1. *Distortion of flow and temperature fields by secondary flow*

When a secondary flow caused by a body force becomes strong in a pipe, the feature of the flow changes considerably from that of a symmetrical flow profile. Profiles of fully developed flow and temperature fields with the secondary flow are shown in Fig. 1.

The stream lines of a weak secondary flow are shown in Fig. 1(A.i) which are obtained by means of the perturbation method from the Navier–Stokes equations [1, 2, 8]. The velocity and temperature distributions obtained by the perturbation method [1, 8] are shown in Fig. 1(A.ii) and (A.iii) respectively. These distributions have only a slight difference from the symmetrical distributions shown by the dashed lines obtained by neglecting secondary flows. Such a slight deviation of profiles is hardly found in experiments.

The growth of a secondary flow to a sufficient extent remarkably distorts velocity and temperature distributions from the symmetrical distributions as shown in Fig. 1(B.ii) and (B.iii). Such distribution profiles were observed in laminar and turbulent flow fields and temperature fields with a secondary flow in curved pipes [6, 7] and in a laminar flow in a heated

horizontal pipe [9]. Influences of viscosity and heat conduction are mainly limited in a thin layer close to the pipe wall; therefore, this layer is called a boundary layer in the sense that the boundary-layer approximation is applicable in this region. On the other hand, the central part of the cross section is called a flow core region, where shearing stress and heat flux by secondary flows are predominant.

Let us consider a body force driving the secondary flow in Fig. 1 which is denoted by X and directs from left to right as shown in the figure. In addition to the pressure gradient along the pipe axis, there exists the pressure distribution in a cross section perpendicular to the axis due to the body force. The pressure distribution in the core region of the cross section is in balance with the body force. Therefore, the secondary flow in the core region is regarded to be such a uniform flow as shown in Fig. 1(B.i). However, in the boundary-layer force balance between the body force and the pressure gradient in a cross section breaks. so that the difference between these forces causes a secondary flow from right to left along the pipe wall as in Fig. 1(B). When the secondary flow is set up, some of the work done by the pressure gradient in the direction of the pipe axis is transferred to the secondary flow, and dissipated by viscous diffusion near the wall. The boundary-layer thickness representing the region of viscous diffusion does not change along the pipe axis in the fully developed flow, where the pressure gradient along the axis is constant, while it changes in a cross section.

1.2. *Fundamental equations*

A system of co-ordinates is shown in Fig. 2. Let $\psi = 0$ be in the direction of the secondary flow in the flow core region; a, the pipe radius: δ, the boundary-layer thickness divided by the pipe radius. Components of velocity in r, ψ and Z direction are denoted by U, V, W respectively; p, pressure; ρ, density and ν, kinematic viscosity.

Dimensionless quantities are defined as follows;

$$\eta = r/a, \quad u = Ua/\nu, \quad v = Va/\nu,$$

$$w = Wa/\nu, \quad z = Z/a, \quad P = (a^2/\nu^2)(p/\rho).$$

As the pressure gradient along the pipe axis in a fully developed flow is constant, we put:

$$\frac{\partial P}{\partial z} = -C \text{ (constant)}.$$

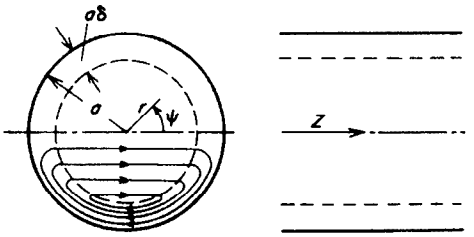

FIG. 2. System of co-ordinates.

When the temperature distribution is fully developed under the condition of a constant wall temperature gradient along the pipe axis, the temperature gradient in the axial (z) direction is constant everywhere in a cross section. Hence, temperature T is expressed in the following form:

$$T = \tau Z - G(r, \psi) \tag{1}$$

where τ is the constant temperature gradient along the pipe axis and $G(r, \psi)$ is a function of r and ψ. Wall temperature T_w is assumed to be constant around the periphery of a cross section, and written thus:

$$T_w = \tau Z. \tag{2}$$

Therefore, the boundary condition of G at the wall is $G = 0$ at $r = a$. Dimensionless temperature g is defined as

$$g = G/\tau a.$$

Heat fluxes in the r and ψ directions and that at the pipe wall are denoted by Q_r, Q_ψ and Q_w respectively, and the dimensionless heat fluxes are defined as follows:

$$q_\eta = Q_r/k\tau, \qquad q_\psi = Q_\psi/k\tau, \qquad q_w = Q_w/k\tau$$

where k is heat conductivity of fluid.

Shearing stresses in the axial direction exerting on a small element of fluid are $\tau_{z\eta}$ and $\tau_{z\psi}$ as shown in Fig. 3. Balance of forces in the z-direction is expressed by the following equation:

$$\frac{\partial}{\eta\partial\eta}(\eta\tau_{z\eta}) + \frac{\partial\tau_{z\psi}}{\eta\partial\psi} = -C. \tag{3}$$

Shearing stresses are

$$\left.\begin{aligned}\tau_{z\eta} &= \frac{\partial w}{\partial\eta} - uw \\ \tau_{z\psi} &= \frac{\partial w}{\eta\partial\psi} - vw.\end{aligned}\right\} \tag{4}$$

The equation of continuity is

$$\frac{\partial}{\eta\partial\eta}(\eta u) + \frac{\partial v}{\eta\partial\psi} = 0. \tag{5}$$

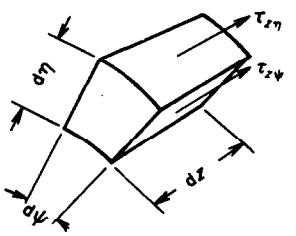

FIG. 3. Shear stresses exerting on a small element of fluid.

From the energy balance of a small element of fluid shown in Fig. 3, the following equation is obtained:

$$\frac{\partial}{\eta\partial\eta}(\eta q_\eta) + \frac{\partial q_\psi}{\eta\partial\psi} = Pr\, w. \tag{6}$$

Heat fluxes are expressed as follows:

$$\left.\begin{aligned}q_\eta &= -\frac{\partial g}{\partial\eta} + Pr\, ug \\ q_\psi &= -\frac{\partial g}{\eta\partial\psi} + Pr\, vg\end{aligned}\right\} \tag{7}$$

where $Pr \equiv \rho c_p \nu/k$ (Prandtl number).

1.3. *The velocity and temperature distributions in the core region*

The suffix 1 is used to denote values in the core region where stresses and heat fluxes due to the secondary flow are predominant. From equations (4) and (7),

$$\tau_{z\eta} = -u_1 w_1, \qquad \tau_{z\psi} = -v_1 w_1 \tag{8}$$

$$q_\eta = Pr\, u_1 g_1, \qquad q_\psi = Pr\, v_1 g_1. \tag{9}$$

Substituting equations (8) and (9) into equations (3) and (6) respectively, we have

$$u_1\frac{\partial w_1}{\partial\eta} + v_1\frac{\partial w_1}{\eta\partial\psi} = C \tag{10}$$

$$u_1\frac{\partial g_1}{\partial\eta} + v_1\frac{\partial g_1}{\eta\partial\psi} = w_1. \tag{11}$$

So as to satisfy these equations and equation (5), u_1, v_1, w_1 and g_1 are expressed as follows:

$$\left.\begin{aligned}u_1 &= D\cos\psi \\ v_1 &= -D\sin\psi \\ w_1 &= A + \frac{C}{D}\eta\cos\psi,\end{aligned}\right\} \tag{12}$$

$$g_1 = A' + \frac{C}{2D^2}\eta^2\cos^2\psi + \frac{A}{D}\eta\cos\psi \tag{13}$$

where A and A' are the constants, and D expresses the dimensionless velocity of the uniform secondary flow in the core region.

The profiles of velocity and temperature, expressed by equations (12) and (13), well approximate the real distributions obtained by the experiments [3, 6, 7, 9]. The profiles of w_1 by equation (12) and g_1 by equation (13) are shown in Fig. 4.

1.4. *The velocity and temperature distributions in the boundary layer*

A distance from the pipe wall is denoted by $\xi(\equiv 1-\eta)$. The assumptions are made that $\delta \ll 1$, and the variation of δ with ψ is quite small. Hereafter, δ is replaced by its peripheral ($\psi = -\pi \sim \pi$) mean value δ_m as the variation of δ with ψ neglected. The value of w_1 at $\xi = \delta$ is denoted by $w_{1\delta}$, and w in the boundary layer joins with $w_{1\delta}$ as shown by dotted lines in Fig. 4. Boundary conditions for w are

at $\xi = 0$ $\quad w = 0$

at $\xi = \delta$ $\quad w = w_{1\delta}$ $\quad \dfrac{\partial w}{\partial \xi} = -\dfrac{\partial w_1}{\partial \eta}$.

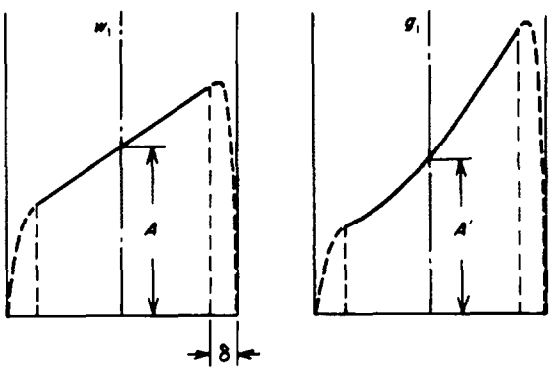

FIG. 4. w_1 and g_1.

To satisfy these conditions, w is written as follows:

$$w = w_{1\delta}\left(2\frac{\xi}{\delta} - \frac{\xi^2}{\delta^2}\right) + \frac{\delta C}{D}\cos\psi\left(\frac{\xi}{\delta} - \frac{\xi^2}{\delta^2}\right). \quad (14)$$

In the expression of the non-dimensional temperature profile in the boundary layer, the influence of Prandtl numbers has to be taken into account. δ and δ_T (dimensionless thermal boundary-layer thickness) are not so clearly defined from a temperature distribution profile obtained by experiments. We denote the ratio of δ_T to δ by $\zeta(=\delta_T/\delta)$, and g_1 at $\xi = \delta$ and δ_T by $g_{1\delta}$ and $g_{1\delta_T}$ respectively.

In the case of $\delta_T \leqslant \delta$, g is expressed so as to satisfy the following boundary conditions:

at $\xi = 0$ $\quad g = 0$

at $\xi = \delta$ $\quad g = g_{1\delta}$ $\quad \dfrac{\partial g}{\partial \xi} = -\dfrac{\partial g_1}{\partial \eta}$.

Satisfying these conditions, we write g in the following form:

$$g = g_{1\delta}\left\{\frac{2}{\zeta}\left(\frac{\xi}{\delta} - 2\frac{\xi^2}{\delta^2} + \frac{\xi^3}{\delta^3}\right) + 3\frac{\xi^2}{\delta^2} - 2\frac{\xi^3}{\delta^3}\right\} + \delta\left\{\frac{C}{D^2}(1-\delta) + \frac{A}{D}\cos\psi\right\}\left(\frac{\xi^2}{\delta^2} - \frac{\xi^3}{\delta^3}\right). \quad (15)$$

In the case of $\delta_T \geqslant \delta$, at $\xi = \delta_T$

$$g = g_{1\delta_T} \quad \frac{\partial g}{\partial \xi} = -\frac{\partial g_1}{\partial \eta}$$

and

$$g = g_{1\delta_T}\left(2\frac{\xi}{\delta_T} - \frac{\xi^2}{\delta_T^2}\right) + \delta_T\left\{\frac{C}{D^2}(1-\delta_T) + \frac{A}{D}\cos\psi\right\}\left(\frac{\xi^2}{\delta_T^2} - \frac{\xi^3}{\delta_T^3}\right). \quad (16)$$

The peripheral velocity component v of the secondary flow in the boundary layer is determined in the following way.

Consider the plane, A–B–O'–B'–A' in a cross section as shown in Fig. 5. The flow rate flowing through the plane, B–O'–B' are equal to those

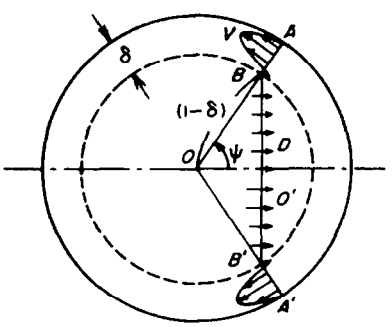

FIG. 5. Secondary flow.

through A–B and B'–A'. This continuous condition of the secondary flow is expressed as

$$\int_0^\delta v\,d\xi = D(1-\delta)\sin\psi. \tag{17}$$

Boundary conditions for v are

at $\xi = 0$ $\quad v = 0$

at $\xi = \delta$ $\quad v = v_1, \quad \dfrac{\partial v}{\partial \xi} = 0.$

In order to satisfy these conditions and equation (17), v is written as follows:

$$v = -D\sin\psi\left[\left(-\frac{12}{\delta}+6\right)\frac{\xi}{\delta}+\left(\frac{24}{\delta}-9\right)\frac{\xi^2}{\delta^2} + \left(-\frac{12}{\delta}+4\right)\frac{\xi^3}{\delta^3}\right]. \tag{18}$$

1.5. *Calculation of A, C and A' in terms of δ, D and ζ*

The mean velocity in a pipe, W_m, is given by the equation

$$W_m = \frac{1}{\pi a^2}\int_{-\pi}^{\pi}\int_0^a W r \quad dr\,d\psi. \tag{19}$$

Dividing the region of integration into the core region and the boundary layer, and using dimensionless quantities, we have from equation (19)

$$w_m \equiv \frac{Re}{2} = \frac{1}{\pi}\left\{\int_{-\pi}^{\pi}\int_0^{1-\delta} w_1\eta\,d\eta\,d\psi + \int_{-\pi}^{\pi}\int_0^{\delta} w(1-\xi)\,d\xi\,d\psi\right\} \tag{20}$$

where $Re = 2aW_m/\nu$ (Reynolds number).

By substituting equations (12) and (14) into equation (20), A is obtained as follows:

$$A = \frac{Re}{2}\frac{1}{1-\frac{2}{3}\delta_m+\frac{1}{6}\delta_m^2}. \tag{21}$$

From the relation of force balance of a fluid element surrounded by a pipe wall and two cross sections as shown in Fig. 6, the following equation is obtained:

$$\int_{-\pi}^{\pi}\int_0^a \frac{\partial p}{\partial Z} r\,dr\,d\psi = \mu\int_{-\pi}^{\pi}\left(\frac{\partial W}{\partial r}\right)_{r=a} a\,d\psi. \tag{22}$$

Use of dimensionless quantities leads from equation (22) to

$$C = \frac{1}{\pi}\int_{-\pi}^{\pi}\left(\frac{\partial w}{\partial \xi}\right)_0 d\psi = 2\left(\frac{\partial w}{\partial \xi}\right)_{0m} \tag{23}$$

where the suffix 0 denotes the value at the pipe wall and m the average value over the periphery.

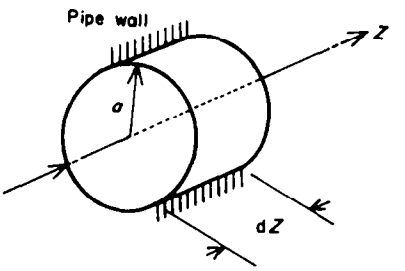

FIG. 6. Portion of fluid under consideration of total force and heat balance.

Substitution of equation (14) in equation (23) gives

$$C = \frac{4A}{\delta_m} = \frac{2Re}{\delta_m}\frac{1}{1-\frac{2}{3}\delta_m+\frac{1}{6}\delta_m^2}. \tag{24}$$

Considering the heat balance of the fluid element shown in Fig. 6, the following equation is obtained;

$$k\int_{-\pi}^{\pi}\left(\frac{\partial T}{\partial r}\right)_{r=a} a\,d\psi = \rho c_p\int_{-\pi}^{\pi}\int_0^a \frac{\partial}{\partial Z}(WT)\,r\,dr\,d\psi. \tag{25}$$

The non-dimensional form of equation (25) is

$$\frac{1}{Pr}\int_{-\pi}^{\pi}\left(\frac{\partial g}{\partial \xi}\right)_0 \mathrm{d}\psi = \int_{-\pi}^{\pi}\int_0^1 w\eta \,\mathrm{d}\eta \,\mathrm{d}\psi = \frac{\pi}{2}Re \qquad (26)$$

or by use of the mean value around the periphery ($\psi = -\pi \sim \pi$), we get

$$\left(\frac{\partial g}{\partial \xi}\right)_{0m} = \frac{Re\,Pr}{4}. \qquad (27)$$

Since δ and δ_T are assumed to be quite small compared with unity, substitution of g given by equations (15) and (16) into equation (27) leads A' for both cases $\delta_T \gtrless \delta$ by eliminating small terms as follows:

$$A' = \frac{\zeta\delta_m RePr}{8} - \frac{Re}{2D^2\delta_m}. \qquad (28)$$

The unknown quantities are now reduced to D, δ_m and ζ included in equations (21), (24) and (28). They are determined from the momentum and energy integral equations of the boundary layer. Among these integral equations, only the equation of momentum in the peripheral direction has the terms including the body force. Therefore, the equations for the unknown quantities, obtained from the equation of momentum in the axial direction and the energy equation, have general applicability to problems pertaining to different body forces.

1.6. *Boundary-layer momentum integral equation in the axial direction*

Equation (4) is substituted into equation (3) and the boundary-layer approximation is made on the basis of the following order estimation:

$$\delta \ll 1, \qquad \eta = 1 - \xi \approx 1,$$
$$(\partial/\partial\eta) = -(\partial/\partial\xi) \sim 0(\delta^{-1}), \qquad u \sim 0(D),$$
$$v \sim 0(D/\delta), \qquad \psi \sim 0(1).$$

The boundary-layer equation becomes

$$-u\frac{\partial w}{\partial \xi} + v\frac{\partial w}{\partial \psi} = C + \frac{\partial^2 w}{\partial \xi^2}. \qquad (29)$$

By integrating this equation about ξ from 0 to δ and arranging it by use of the equation of continuity $(\partial u/\partial\xi) = (\partial v/\partial\psi)$, the following boundary-layer momentum integral equation is obtained:

$$\left(\frac{\partial w}{\partial \xi}\right)_0 = w_{1\delta}\frac{\partial}{\partial\psi}\int_0^\delta v\,\mathrm{d}\xi - \frac{\partial}{\partial\psi}\int_0^\delta vw\,\mathrm{d}\xi + C\delta. \qquad (30)$$

Substituting equations (14) and (18) into the right-hand side of equation (30) and integrating them, we have

$$\left(\frac{\partial w}{\partial \xi}\right)_0 = E + F\cos\psi \qquad (31)$$

where

$$E = \left\{\left(\frac{2}{5} - \frac{13}{15}\delta_m\right)\cos^2\psi + \left(\frac{3}{5} - \frac{17}{15}\delta_m\right)\sin^2\psi + \delta_m\right\}C \qquad (32)$$

$$F = \frac{D\delta_m}{4}\left(\frac{2}{5} - \frac{4}{15}\delta_m\right)C. \qquad (33)$$

The mean value of $(\partial w/\partial\xi)_0$ around the periphery ($\psi = -\pi \sim \pi$) obtained from equation (31) obviously satisfies equation (23). The terms contributing to the mean value are grouped in E as seen from equation (32), and they vary with ψ through $\cos^2\psi$ and $\sin^2\psi$; however, the variation of E by ψ is so little in comparison with $F\cos\psi$ that E may be replaced by the mean value $C/2$ [6].

Thus, we have

$$\left(\frac{\partial w}{\partial \xi}\right)_0 = \frac{C}{2} + F\cos\psi. \qquad (34)$$

On the other hand, the gradient $(\partial w/\partial\xi)_0$ is also written from equation (14) that

$$\left(\frac{\partial w}{\partial \xi}\right)_0 = w_{1\delta}\frac{2}{\delta} + \frac{C}{D}\cos\psi = \frac{C}{2} + \left(\frac{2}{\delta_m} - 1\right)\frac{C}{D}\cos\psi. \qquad (35)$$

By equating equations (34) and (35), we get the following relation about D and δ_m

$$(1 - \tfrac{2}{3}\delta_m) D^2\delta_m^2 + 10\delta_m = 20. \quad (36)$$

In order to increase the accuracy of the boundary-layer approximation, D and δ_m are expanded in successive series by the particular non-dimensional parameter. For example, in the analysis of a laminar flow in a curved pipe [6], it is expanded by $-\frac{1}{2}$ power series of Dean number $K[= Re(\sqrt{a/R}), R$, radius of curvature of pipe axis] as follows:

$$\left.\begin{aligned} D &= D_1K^{\frac{1}{2}} + D_2 + D_3K^{-\frac{1}{2}} + \dots \\ \delta_m &= \delta_{m1}K^{-\frac{1}{2}} + \delta_{m2}K^{-1} + \dots . \end{aligned}\right\} \quad (37)$$

By substituting equation (37) into equation (36) and equating the terms having the same power of K, algebraical equations about D_1, δ_{m1}, D_2, δ_{m2} ... are obtained successively. However, in the following analysis only the first approximation is analysed.

Equations concerning the first approximation are shown below. From equation (21)

$$A = \frac{Re}{2}. \quad (38)$$

From equation (24)

$$C = \frac{2Re}{\delta_m}. \quad (39)$$

From equation (36)

$$D^2\delta_m^2 = 20. \quad (40)$$

1.7. *Energy integral equation of boundary layer*

By substituting equation (7) into equation (6) and applying the boundary-layer approximation, we have the following energy equation of the boundary layer:

$$-\frac{1}{Pr}\frac{\partial^2 g}{\partial \xi^2} - u\frac{\partial g}{\partial \xi} + v\frac{\partial g}{\partial \psi} - w = 0. \quad (41)$$

(1) *In the case of* $\delta_T \leqslant \delta$. Equation (41) is integrated with ξ from 0 to δ and the following energy integral equation is obtained:

$$\frac{1}{Pr}\left(\frac{\partial g}{\partial \xi}\right)_0 = g_{1\delta}\frac{\partial}{\partial \psi}\int_0^\delta v\,d\xi - \frac{\partial}{\partial \psi}\int_0^\delta gv\,d\xi + \int_0^\delta w\,d\xi. \quad (42)$$

Following the same procedure described in the previous section, ζ is obtained from equation (42). As shown in equation (13), g_1 has a non-linear distribution about $\cos\psi$. Therefore, proceeding in the same way of calculation about the flow field, $g_{1\delta}$ is assumed as

$$g_{1\delta} = A' + \frac{C}{4D^2}(1-\delta)^2 + \frac{A}{D}(1-\delta)\cos\psi \approx \frac{\zeta\delta_m Re\,Pr}{8} + \frac{Re}{2D}\cos\psi. \quad (43)$$

Equations (14), (15) and (18) are substituted into the right-hand side of equation (42). Elimination of small quantities yields

$$\left(\frac{\partial g}{\partial \xi}\right)_0 = E' + F'\cos\psi \quad (44)$$

where

$$E' = \frac{Re\,Pr}{2}\left\{\left(\frac{22}{35} - \frac{8}{35\zeta}\right)\cos^2\psi + \left(\frac{13}{35} + \frac{8}{35\zeta}\right)\sin^2\psi\right\} \quad (45)$$

$$F' = \frac{\zeta D\delta_m Re\,Pr^2}{8}\left(\frac{22}{35} - \frac{8}{35\zeta}\right). \quad (46)$$

The convective term due to w in equation (42) can be disregarded, since it is small compared with the other terms.

As it is clear from equation (45), the mean value of $(\partial g/\partial \xi)_0$ in equation (44) satisfies equation (27). As the variation of E' with ψ is small compared with $F'\cos\psi$, equation (44) is expressed as

$$\left(\frac{\partial g}{\partial \xi}\right)_0 = \frac{Re\,Pr}{4} + F'\cos\psi. \quad (47)$$

On the other hand, from equation (15) we have

$$\left(\frac{\partial g}{\partial \xi}\right)_0 = \frac{2}{\zeta \delta_m} g_{1\delta} = \frac{Re\,Pr}{4} + \frac{Re}{\zeta D \delta_m} \cos\psi. \quad (48)$$

When we equate equations (47) and (48), for $Pr \geqslant 1$ we obtain the following relation ($\zeta \leqslant 1$) as

$$\zeta = \frac{2}{11}\left[1 + \sqrt{\left(1 + \frac{77}{4}\frac{1}{Pr^2}\right)}\right] \quad (49)$$

(2) *In the case of* $\delta_T \geqslant \delta$. In this case, integration of the boundary-layer equation should be done by dividing the region into $\xi = 0 \sim \delta$ and $\delta \sim \delta_T$. By calculating the integration of (42) by use of g given by equation (16) we have

$$\left(\frac{\partial g}{\partial \xi}\right)_0 = \frac{Re\,Pr}{4} + \frac{\zeta D \delta_m\, Re\, Pr^2}{8} \times \left(1 - \frac{4}{5\zeta} + \frac{1}{5\zeta^2}\right)\cos\psi. \quad (50)$$

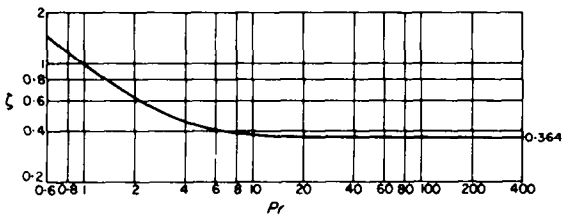

FIG. 7. ζ vs. Pr.

From equation (16), the gradient $(\partial g/\partial \xi)_0$ is written in the same expression as equation (48) when Pr is not much different from unity. By equating equations (48) and (50), for $Pr \leqslant 1$ we obtain the relations (for $\zeta \geqslant 1$) as

$$\zeta = \frac{1}{5}\left[2 + \sqrt{\left(\frac{10}{Pr^2} - 1\right)}\right]. \quad (51)$$

The ratio ζ calculated by equations (49) and (51) is shown in Fig. 7.

1.8. *Resistance coefficient and Nusselt numbers*

Resistance coefficient λ and Nusselt number Nu are defined as

$$\lambda = \left(-\frac{\partial p}{\partial Z}\right)\frac{2a}{\frac{1}{2}\rho W_m^2} \quad (52)$$

$$Nu = \frac{2aQ_{wm}}{k(T_w - T_m)} \quad (53)$$

where Q_{wm} is the mean heat flux at the wall around the periphery of a cross section ($\psi = -\pi \sim \pi$), and T_m is the mixed mean temperature:

$$T_m = \frac{1}{\pi a^2 W_m}\int_{-\pi}^{\pi}\int_0^a TWr\,dr\,d\psi. \quad (54)$$

Non-dimensional mixed mean temperature g_m is written as

$$g_m \equiv \frac{T_w - T_m}{\tau a} \approx \frac{2}{\pi\, Re}\int_{-\pi}^{\pi}\int_0^1 g_1 w_1 \eta\,d\eta\,d\psi = \frac{\zeta\, Re\, Pr}{8}\delta_m + \frac{1}{4}\frac{Re}{D^2\delta_m}. \quad (55)$$

The resistance coefficient for the Poiseuille velocity distribution is

$$\lambda_0 = \frac{64}{Re} \quad (56)$$

and Nusselt number for symmetrical temperature distribution and constant heat flux is

$$Nu_0 = \frac{48}{11}. \quad (57)$$

The ratio of λ to λ_0 and that of Nu to Nu_0 are expressed as follows by use of the dimensionless quantities:

$$\frac{\lambda}{\lambda_0} = \frac{C}{4Re} = \frac{1}{2\delta_m} = \frac{D}{2\sqrt{20}} \quad (58)$$

$$\frac{Nu}{Nu_0} = \frac{11}{48}\frac{Re\,Pr}{2g_m} = \frac{11}{12}\frac{1}{\zeta\delta_m}\frac{1}{1 + [1/(10\zeta\, Pr)]} = \frac{11}{12\sqrt{20}}\frac{D}{\zeta}\frac{1}{1 + [1/(10\zeta\, Pr)]}. \quad (59)$$

2. HEAT TRANSFER IN A STRAIGHT PIPE ROTATING ABOUT A PARALLEL AXIS

The particular relation between D and δ_m for the present problem is given by the equations of force balance in the r and ψ direction. The body force driving the secondary flow is caused by density difference in the centrifugal field, and the Coriolis force has a little influence on the flow and temperature fields.

2.1. *Fundamental equations*

The pipe axis rotates about an axis with an angular velocity ω as shown in Fig. 8. The angle measured from the line passing through the center of a cross section and the axis of rotation is denoted by ψ'. Because of the Coriolis' force, ψ' does not necessarily agree with ψ which is measured from the direction of the secondary flow in the core region. The angle of deviation due to Coriolis force is denoted by $\Delta = \psi - \psi'$.

The expressions of acceleration in the η and ψ directions in a cross section are

$$a_{cc.\eta} = u\frac{\partial u}{\partial \eta} + \frac{v}{\eta}\frac{\partial u}{\partial \psi} - \frac{v^2}{\eta} - Jv - \frac{a^4}{\nu^2}H\omega^2\left(\cos\psi' + \frac{\eta}{H}\right) \quad (60)$$

$$a_{cc.\psi} = u\frac{\partial v}{\partial \eta} + \frac{v}{\eta}\frac{\partial v}{\partial \psi} + \frac{uv}{\eta} + Ju + \frac{a^4}{\nu^2}H\omega^2\sin\psi' \quad (61)$$

where J is the parameter relating the Coriolis effect $J = 2a^2\omega/\nu$ and H is the distance between the pipe axis and the rotation axis.

The last terms in the right-hand side in equations (60) and (61) express centrifugal force caused by rotation.

When the fluid and the pipe wall are kept at the same temperature, there is no body force to drive a secondary flow, and we have the following pressure distribution

$$P_0 = \frac{a^4}{\nu^2}H\omega^2\eta\left(\cos\psi' + \frac{\eta}{2H}\right) + P_c \quad (62)$$

where P_c is the pressure at the pipe axis. When a temperature distribution exists in the cross section, the secondary flow occurs due to buoyancy, and P_0 comes to deviate from P_0 given by equation (62). The deviation of pressure from P_0 is newly denoted by P hereafter, so that non-dimensional pressure is $P_0 + P$.

When ω is very large, the fluid is subjected to a strong centrifugal acceleration many times larger than the gravitational one. The effect

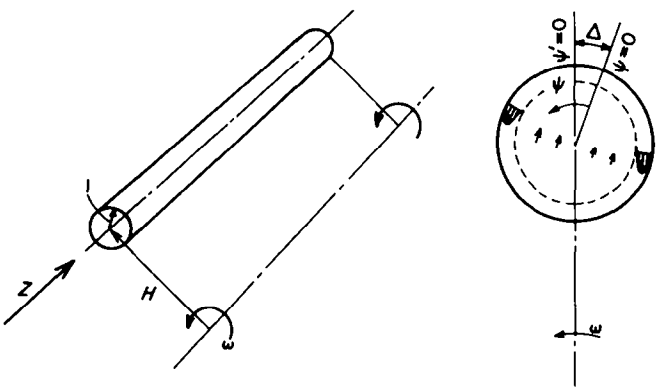

FIG. 8. Co-ordinates of a rotating pipe.

of body force is expressed in terms of density change in the centrifugal field; therefore, the following Grashoff number for the centrifugal field is introduced:

$$Gr = \frac{(aH)\omega^2\beta\tau a^4}{\nu^2}$$

where β is the coefficient of volumetric expansion.

The equations of motion are written as

$$u\frac{\partial u}{\partial \eta} + \frac{v}{\eta}\frac{\partial u}{\partial \psi} - \frac{v^2}{\eta} - Jv = -\frac{\partial P}{\partial \eta} + \nabla^2 u - \frac{u}{\eta^2} - \frac{2}{\eta^2}\frac{\partial v}{\partial \psi} + Gr\, g\cos\psi' \quad (63)$$

$$u\frac{\partial v}{\partial \eta} + \frac{v}{\eta}\frac{\partial v}{\partial \psi} + \frac{uv}{\eta} + Ju = -\frac{\partial P}{\eta \partial \psi} + \nabla^2 v + \frac{2}{\eta^2}\frac{\partial u}{\partial \psi} - \frac{v}{\eta^2} - Gr\, g\sin\psi' \quad (64)$$

where

$$\nabla^2 \equiv \frac{\partial^2}{\partial \eta^2} + \frac{1}{\eta}\frac{\partial}{\partial \eta} + \frac{1}{\eta^2}\frac{\partial^2}{\partial \psi^2}.$$

2.2. *The core region*

By use of equation (12) the force balance equations in the core region are written from equations (63) and (64) as

$$\frac{\partial P_1}{\partial \eta} = -JD\sin(\psi' + \Delta) + Gr\, g_1\cos\psi' \quad (65)$$

$$\frac{\partial P_1}{\eta \partial \psi} = -JD\cos(\psi' + \Delta) - Gr\, g_1\sin\psi'. \quad (66)$$

When P_1 is eliminated from equations (65) and (66),

$$\cos\psi'\frac{\partial g_1}{\eta \partial \psi} + \sin\psi'\frac{\partial g_1}{\partial \eta} = 0. \quad (67)$$

The dimensionless temperature g_1 given by equation (13) satisfies equation (67) when the effect of Coriolis' force is small and $\psi \approx \psi'$.

2.3. *Boundary-layer momentum integral equation in the peripheral direction*

We have the boundary-layer equation from equations (63) and (64) as follows:

$$-v^2 - Jv = \frac{\partial P}{\partial \xi} + Gr\, g\cos\psi' \quad (68)$$

$$-u\frac{\partial v}{\partial \xi} + v\frac{\partial v}{\partial \psi} + Ju = -\frac{\partial P}{\partial \psi} + \frac{\partial^2 v}{\partial \xi^2} - Gr\, g\sin\psi'. \quad (69)$$

Pressure P in the boundary layer is written as

$$P = P_{1\delta} + \int_{\xi}^{\delta}(v^2 + Jv + Gr\, g\cos\psi')\,d\xi \quad (70)$$

where $P_{1\delta}$ is the value of P_1 at $\xi = \delta$.

The integration in the right-hand side of equation (70) is small compared with $P_{1\delta}$, thus

$$P \approx P_{1\delta}. \quad (71)$$

From the integration of equation (69) with ξ from 0 to δ, we obtain the boundary-layer momentum integral equation in the peripheral direction as

$$\left(\frac{\partial v}{\partial \xi}\right)_0 = v_1\frac{\partial}{\partial \psi}\int_0^{\delta} v\,d\xi - \frac{\partial}{\partial \psi}\int_0^{\delta} v^2\,d\xi - J\int_0^{\delta} u\,d\xi - \delta\frac{dP_{1\delta}}{d\psi} - Gr\int_0^{\delta} g\sin\psi'\,d\xi. \quad (72)$$

The first and second terms in the right-hand side of equation (72) express incoming and outgoing momentum flux from the control volume of the boundary layer. They are due to the variation of δ along the periphery and the third term expresses the effect of the Coriolis force. As discussed for flows in a curved pipe [6], δ does not deviate remarkably from δ_m [6], and in the first approximation we may disregard the first and second integrals of equation (72). The effect of the Coriolis force will be investigated in detail later.

For this reason, we take the mean of both sides of equation (72) between $\psi = 0 \sim \pi$.

The following equation thus obtained is the fundamental relation:

$$\left(\frac{\partial v}{\partial \xi}\right)_{0m} = -\delta_m\left(\frac{dP_{1\delta}}{d\psi}\right)_m - Gr\left(\int_0^\delta g \sin\psi' \, d\xi\right)_m. \tag{73}$$

It is expected by referring to the author's analysis for flows in a curved pipe [6] that δ_m determined in this way is almost equal to that calculated in the detailed analysis to the second approximation.

From equation (66):

$$\left(\frac{dP_{1\delta}}{d\psi}\right)_m = -Gr(g_{1\delta}\sin\psi')_m. \tag{74}$$

For simplicity, we write non-dimensional temperature g as

$$g = g_{1\delta}\, h(\lambda/\delta) \tag{75}$$

where h is the polynomial of ξ/δ in equation (15) or (16).

Moreover, by putting

$$1 - \frac{1}{\delta_m}\int_0^\delta h \, d\xi = b \tag{76}$$

equation (73) is expressed as

$$\left(\frac{\partial v}{\partial \xi}\right)_{0m} = Gr\,\delta_m b(g_{1\delta}\sin\psi')_m. \tag{77}$$

When $\psi' \approx \psi$, substitution of equations (18) and (43) into equation (77) yields

$$12\frac{D}{\delta_m^2} = b\frac{\zeta}{8}Ra_r Re\,\delta_m^2 \tag{78}$$

where $Ra_r = Gr \,.\, Pr$ (Rayleigh number for the centrifugal field). From equations (40) and (78), D is obtained as

$$D = \left(\frac{25b\zeta}{6}\right)^{\frac{1}{4}}(Ra_r Re)^{\frac{1}{4}} \tag{79}$$

where b is obtained by using equation (15) or (16).

For $Pr \geqslant 1$ ($\zeta \leqslant 1$),

$$D = 0{\cdot}930\,(3\zeta - 1)^{\frac{1}{4}}(Ra_r Re)^{\frac{1}{4}} \tag{80}$$

where $\zeta > 0{\cdot}364$ as shown in Fig. 7.

For $Pr \leqslant 1$ ($\zeta \geqslant 1$),

$$D = 1{\cdot}330\left(\zeta - 1 + \frac{1}{3\zeta}\right)^{\frac{1}{4}}(Ra_r Re)^{\frac{1}{4}}. \tag{81}$$

2.4. *Resistance coefficients and Nusselt numbers*

Substitution of equations (80) and (81) into equations (58) and (59) gives λ/λ_0 and Nu/Nu_0 as follows:

for $Pr \geqslant 1$:

$$\frac{\lambda}{\lambda_0} = 0{\cdot}104\,(3\zeta - 1)^{\frac{1}{4}}(Ra_r Re)^{\frac{1}{4}} \tag{82}$$

$$\frac{Nu}{Nu_0} = \frac{0{\cdot}191}{\zeta}(3\zeta - 1)^{\frac{1}{4}}(Ra_r Re)^{\frac{1}{4}} \times \frac{1}{1 + [1/(10\zeta\, Pr)]} \tag{83}$$

for $Pr \leqslant 1$:

$$\frac{\lambda}{\lambda_0} = 0{\cdot}149\left(\zeta - 1 + \frac{1}{3\zeta}\right)^{\frac{1}{4}}(Ra_r Re)^{\frac{1}{4}} \tag{84}$$

$$\frac{Nu}{Nu_0} = \frac{0{\cdot}273}{\zeta}\left(\zeta - 1 + \frac{1}{3\zeta}\right)^{\frac{1}{4}}(Ra_r Re)^{\frac{1}{4}} \times \frac{1}{1 + [1/(10\zeta\, Pr)]}. \tag{85}$$

In Fig. 9, the theoretical results given by equations (83) and (85) are shown by the solid straight lines. The curved line on the left in Fig. 9 is drawn from Morris' analytical results [1] taking into account the terms of the second order of magnitude, but it shows the rapid divergence of the solution with increasing $Ra_r Re$.

2.5. *The effect of Coriolis' force*

Effects of Coriolis' force appear through the angle of deviation Δ in the present analysis. Considering that the line $\psi = 0$ is the line of symmetry in the flow field, we put it as follows

in equation (66) to obtain Δ: $\eta \approx 1$, $dP_{1\delta}/d\psi = 0$, $\psi = 0$, $\psi' = -\Delta$. The deviation angle is given by

$$\sin \Delta = \frac{1}{\zeta \sqrt{20/8 + (Ra_r Re/2Pr)}} \frac{JD^2}{}. \quad (86)$$

When Δ is taken into account in obtaining the mean value,

$$(g_{1\delta} \sin \psi')_m = \frac{1}{4\pi} \zeta \delta_m Re\, Pr \cos \Delta - \frac{Re}{4D} \sin \Delta. \quad (87)$$

By putting $\cos \Delta \approx 1$ and $\sin \Delta \approx \Delta$ in equation (87) and using equation (86), the equation corresponding to equation (79) is written as

$$D^5 + \frac{25\pi b}{3(\sqrt{5})\,[\zeta\, Pr\,(\sqrt{5}) + 2]} JD^2 = \frac{25b\zeta}{6} (Ra_r Re). \quad (88)$$

The second term of the left-hand side in equation (88) is presumed to be small.

Therefore, we put

$$D = D_1 + D_2$$

where D_1 is that given by equation (79). Assuming $D_1 \gg D_2$, we have from equation (88)

$$D_2 = -\frac{5\pi b}{3(\sqrt{5})\,[\zeta\, Pr\,(\sqrt{5}) + 2]} \frac{J}{D_1^2}. \quad (89)$$

From equations (79) and (89), D is determined as follows:

for $Pr \geqslant 1$

$$D = 0{\cdot}930\,(3\zeta - 1)^{\frac{1}{5}} (Ra_r Re)^{\frac{1}{5}} \left\{1 - 0{\cdot}486 \frac{(3\zeta - 1)^{\frac{2}{5}}}{\zeta[\zeta\, Pr\,(\sqrt{5}) + 2]} \frac{J}{(Ra_r Re)^{\frac{1}{5}}}\right\} \quad (90)$$

for $Pr \leqslant 1$

$$D = 1{\cdot}330 \left(\zeta - 1 + \frac{1}{3\zeta}\right)^{\frac{1}{5}} (Ra_r Re)^{\frac{1}{5}} \left\{1 - 0{\cdot}995 \frac{[\zeta - 1 + (1/3\zeta)]^{\frac{2}{5}}}{\zeta[\zeta\, Pr\,(\sqrt{5}) + 2]} \frac{J}{(Ra_r Re)^{\frac{1}{5}}}\right\}. \quad (91)$$

Therefore, when the effect of Coriolis' force cannot be disregarded, it is recommended to multiply λ/λ_0 and Nu/Nu_0 of equations (82–85) by the correction coefficients which are calculated from the terms closed in the brackets in equations (90) and (91). The broken lines shown in Fig. 9 are Nu/Nu_0 including the effect of Coriolis' force, which is expressed by non-dimensional parameter J.

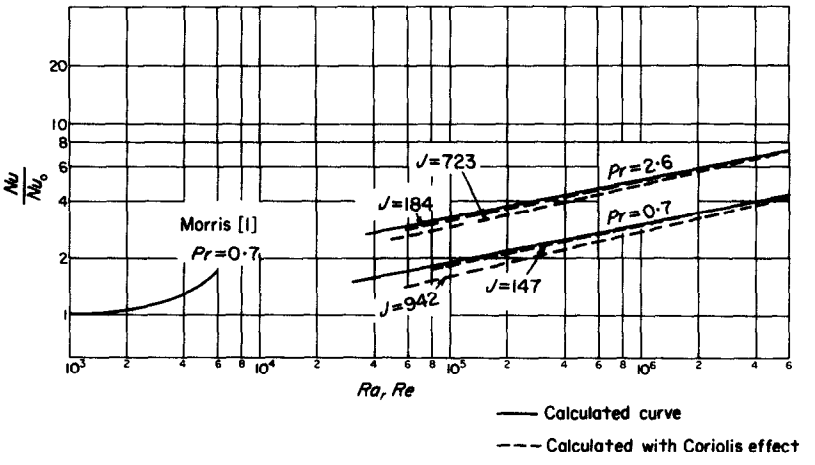

FIG. 9. Theoretical curves of Nu/Nu_0 vs. $Ra_r Re$.

It is clear from equation (66) that the increase in Δ decreases the pressure gradient driving the secondary flow, so that the dimensionless velocity D of the secondary flow decreases as shown in equations (90) and (91). The increase in Coriolis' force lessens flow resistance and heat-transfer rate as shown in Fig. 9. When we put the rotating velocity of the pipe axis $H\omega = \alpha$, the correction coefficients in equations (90) and (91) are proportional to $\omega^{\frac{1}{2}}/\alpha^{\frac{1}{2}}$. Keeping α constant, we can conclude that the effect of Coriolis' force becomes large in a pipe with a small radius of rotation.

CONCLUSIONS

Fully developed laminar flow and temperature fields in a straight pipe rotating about a parallel axis are analysed under a constant wall temperature gradient condition, and the following conclusive results are obtained.

(1) In order to make the analytical results available for practical use, flow and temperature fields can be analysed by assuming a secondary flow and dividing the fields into a core region, where the effect of the secondary flow is predominant, and a boundary layer along the wall. Since the momentum equation in the direction of the pipe axis and the energy equation do not explicitly contain the terms of body force, the relations obtained from them may generally be used between unknown quantities in the analysis of convective heat transfer in a pipe with a secondary flow generated by various body forces.

(2) The specific relation for the present problem is obtained from the momentum equation in the circumferential direction which expresses force balance between the body force in the strong centrifugal field and viscous resistance against the secondary flow at the pipe wall.

(3) The resistance coefficient ratio λ/λ_0 ($\lambda_0 = 64/Re$ for Poisieulle profile) and the Nusselt number ratio Nu/Nu_0 ($Nu_0 = 48/11$ for constant temperature gradient) are obtained as the functions of Pr and $Ra_r Re$. They are proportional to $(Ra_r Re)^{\frac{1}{2}}$ in the region of large values of $Ra_r Re$, when the Coriolis' effect is disregarded.

(4) It is shown that the effect of Coriolis' force appears through the non-dimensional parameter $J(= 2a^2\omega/\nu)$.

The correction coefficients are given by taking into account this effect in the evaluation of λ/λ_0 and Nu/Nu_0. When the circumferential velocity of the pipe axis is kept constant, the decrease in a radius of rotation increases the Coriolis' effect, which lessens both the pressure drop and the heat-transfer rate.

REFERENCES

1. W. D. Morris, Laminar convection in a heated vertical tube rotating about a parallel axis, *J. Fluid Mech.* **10**, 453 (1965).
2. W. R. Dean, Note on the motion of fluid in a curved pipe, *Phil. Mag.* **4**, 208 (1927); *Phil. Mag.* **5**, 673 (1928).
3. M. Adler, Strömung in gekrümmten rohren, *Z. Angew. Math. Mech.* **14**, 257 (1934).
4. S. N. Barua, On secondary flow in stationary curved pipes, *Q. Jl Mech. Appl. Math.* **16**, 61 (1962).
5. H. Ito, Friction factors for turbulent flow in curved pipes, *J. Bas. Engng* **81D**, 123 (1959).
6. Y. Mori and W. Nakayama, Study on forced convective heat transfer in curved pipes (1st report, laminar region) *Int. J. Heat Mass Transfer* **8**, 67 (1965).
7. Y. Mori and W. Nakayama, Study on forced convective heat transfer in curved pipes (2nd report, turbulent region), *Int. J. Heat Mass Transfer* **10**, 37 (1967).
8. B. R. Morton, Laminar convection in uniformly heated horizontal pipes at low Rayleigh numbers, *Q. Jl Mech. Appl. Math.* **12**, 410 (1959).
9. Y. Mori, K. Futagami, S. Tokuda and M. Nakamura, Forced convective heat transfer in uniformly heated horizontal tubes, 1st report—experimental study on the effect of buoyancy, *Int. J. Heat Mass Transfer* **9**, 453 (1966).
10. Y. Mori and K. Futagami, Forced convective heat transfer in uniformly heated horizontal tubes, 2nd report—theoretical study on the effect of buoyancy, *Trans. Japan. Soc. Mech. Engrs* **32**, 88 (1966).

Résumé— Le transport de chaleur par convection forcée dans un tuyau rectiligne tournant autour d'un axe parallèle avec und grande vitesses angulaire a été étudié en supposant un écoulement secondaire effectif dû aux forces d'Archimède. Les problèmes de transport de chaleur étudiés ici se posent habituellement lorsqu'on refroidit les générateurs électriques ou d'autres machines tournantes. Les champs d'écoulement et de température sont analysés en les divisant en une région centrale et une couche limite mince le long de la paroi. L'analyse d'un écoulement laminaire entièrement établi dans le cas d'un gradient de

température pariétale constant consiste en deux parties. La première est une partie commune à de nombreux problèmes avec écoulements secondaires et la deuxième contient des points particuliers au problème actuel. Les résultats montrent que le rapport des coefficients de résistance et celui des nombres de Nusselt aux valeurs de l'écoulement de Poiseuille sont proportionnels à $(Ra_r . Re)^{\frac{1}{2}}$; ($Ra_r$: nombre de Rayleigh pour le champ centrifuge, Re: nombre de Reynolds). On donne également les coefficients de correction dus à l'effet Coriolis.

Zusammenfassung—Es wurde der Wärmeübergang bei erzwungener Konvektion in einem geraden Rohr, das um eine parallele Achse mit grosser Winkelgeschwindigkeit rotiert unter der Annahme einer wirksamen Zweitströmung infolge des Auftriebs untersucht. Die hier betrachteten Wärmeübergangsprobleme finden sich häufig bei der Kühlung elektrischer Generatoren oder anderer rotierender Maschinen. Strömungs- und Temperaturfeld werden analysiert, indem man sie in eine Kernströmung und eine dünne Grenzschicht entlang der Wand unterteilt. Die Analyse der voll ausgebildeten Laminarströmung bei konstantem Gradienten der Wandtemperatur wird hier in zwei Teilen behandelt. Der erste Teil gibt die für verschiedene Probleme mit Zweitströmung begräuchliche Betrachtung, der zweite Teil umfasst besonders Fragen des gegenwärtigen Problems. Das Ergebnis zeigt, dass das Verhältnis sowohl der Widerstandskoeffizienten als auch der Nusselt–Zahlen zum Wert der Poiseuille-Strömung proportional $(Ra_r . Re)^{\frac{1}{2}}$ ist. (Ra_r: Rayleigh-Zahl im Zentrifugalfeld, Re: Reynolds-Zahl). Korrekturkoeffizienten zur Berücksichtigung des Coriolis-effektes sind angegeben.

Аннотация—Исследован вынужденный конвективный теплообмен в прямой трубе, вращающейся вокруг параллельной оси с большой угловой скоростью в допущении эффективного вторичного течения вследствие подъемных сил, обусловленных градиентом плотности. При охлаждении электрогенераторов и других вращающихся машин обычно сталкиваются с проблемами теплообмена, рассмотренными в этой статье. Анализируются скоростные и температурные поля путем разделения их на ядро потока и на тонкий пограничный пристеночный слой. Две части этого доклада содержат анализ полностью развитого ламинарного потока в условиях постоянного градиента температуры стенки. Первая часть общая для различных задач с вторичными течения, а вторая часть содержит частные задачи. Результат показывает, что отношения друг к другу коэффициентов сопротивления, а также чисел Нуссельта в условиях Пуазейлевого течения пропорциональны $(Ra_r \cdot Re)^{\frac{1}{2}}$ (Ra_r, число Релея в центробежном поле; Re, число Рейнолдьса). Даются также поправочные коэффициенты Кориолисового эффекта.